

The Importance of Fluctuations in Fluid Mixing

Kai Kadau, John L. Barber, Timothy C. Germann, T-14; Pierre Carlès, Université Paris; Berni J. Alder, Lawrence Livermore National Laboratory; Charles Rosenblatt, Zhibin Huang, Case Western Reserve Univ.

A ubiquitous example of fluid mixing is the Rayleigh-Taylor instability, in which a heavy fluid initially sits atop a light fluid in a gravitational field. The subsequent development of the unstable interface between the two fluids is marked by several stages. At first, each interface mode grows exponentially with time, before transitioning to a nonlinear regime characterized by more complex hydrodynamic mixing. Unfortunately, traditional continuum modeling of this process has generally been in poor agreement with experiment. Here we indicate that the natural, random fluctuations of the flow field present in any fluid, which are neglected in continuum models, can lead to qualitatively and quantitatively better agreement with experiment. We performed billion-particle atomistic simulations with the LANL SPaSM code and magnetic levitation experiments with unprecedented control of initial interface conditions. A comparison between our simulations and experiments reveals good agreement in terms of the growth rate of the mixing front, as well as the new observation of droplet breakup at later times. These results improve our understanding of many fluid processes, including interface phenomena that occur, for example, in supernovae, the detachment of droplets from a faucet, and inkjet printing. Such instabilities are also relevant to inertial confinement fusion (ICF), in which a millimeter-sized capsule is imploded to increase pressure and temperature, and initiate nuclear fusion reactions between deuterium and tritium. An understanding of the flow in such an imploding capsule is necessary to achieve a cleaner source of energy than the ordinary fission reactions used in today's nuclear power plants. Overall, our results suggest that the applicability of continuum models would be greatly enhanced by explicitly including the effects of random fluctuations.

For more information contact Kai Kadau at kkadau@lanl.gov.

Reference

K. Kadau et al., *Proc. Natl. Acad. Sci. USA*, **104**, 7741-7745 (2007).

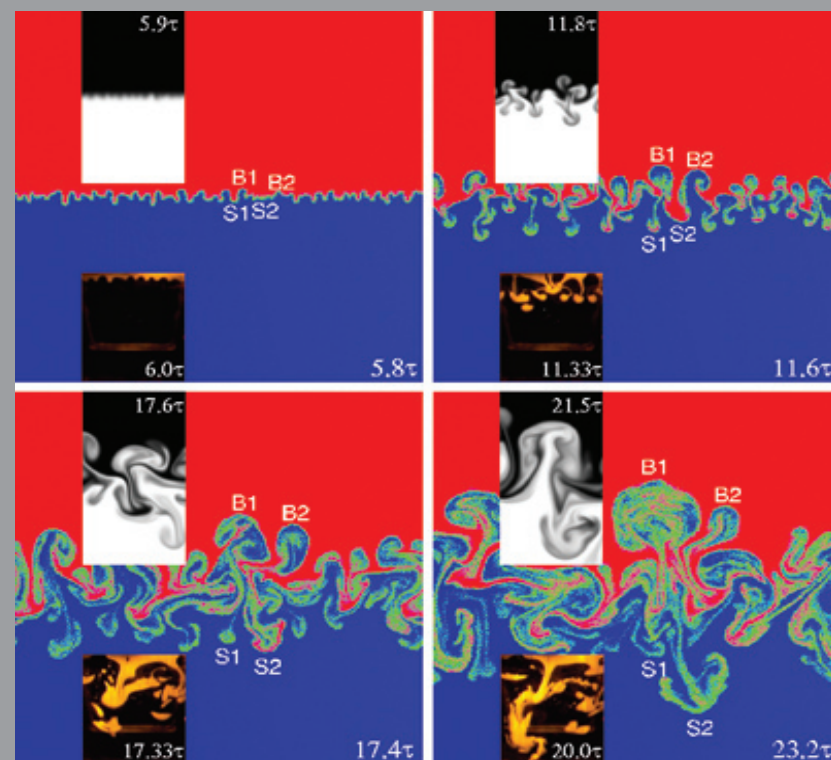


Fig.1. Time evolution of RT instability. Atomistic simulation of a 2D RT instability employing 570 million DSMC particles, where the heavy fluid (red) is on top of the light fluid (blue), and the gravitational field points downwards ($A=0.67$). The initially flat interface roughens due to thermal fluctuations, and modes near the most unstable mode develop first. Later, merger processes become dominant. At even later times, breakups occur that reduce the overall growth of the mixing layer. The position of individual spikes (S1, S2) and bubbles (B1, B2) shows the variation of movement and development of individual spikes and bubbles. Macroscopic magnetic levitation 2D RT experiments (color insets, showing only the spikes in orange, system width 7cm, $\tau=0.05$ sec, $A=0.29$) exhibit similar breakups. For comparison, a cutout from a 2D continuum simulation is shown (grayscale inset, $A=0.5$) (24). The outer scale Reynolds-numbers at the last frame for the atomistic simulation, experiment, and continuum simulation are 2200, 3000, and 1800, respectively.

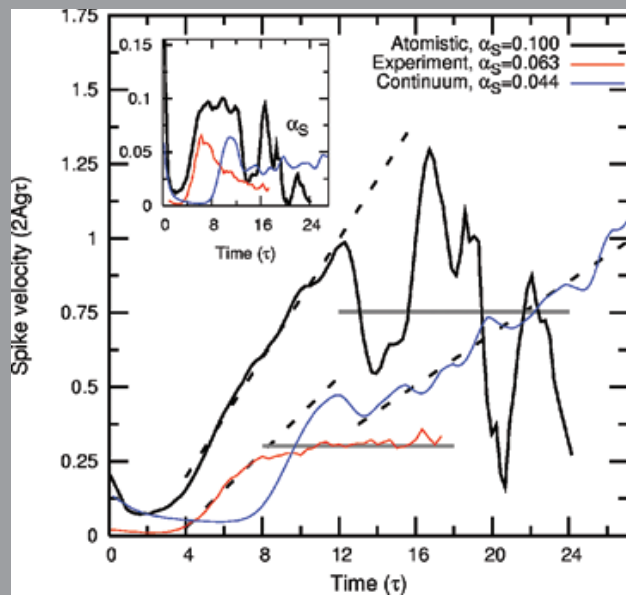


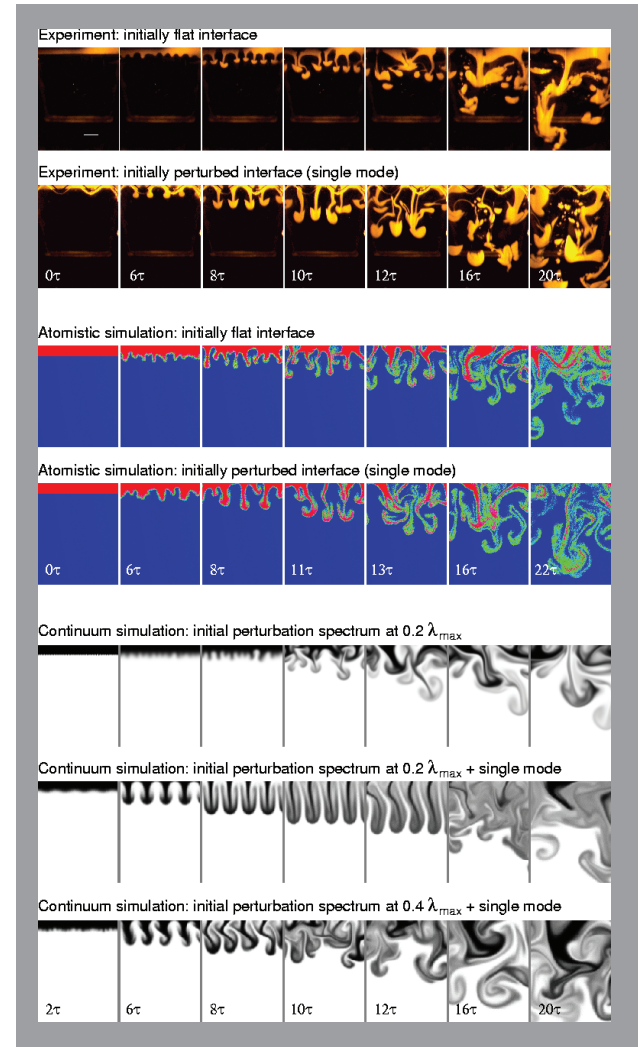
Fig. 2. Spike velocity. Spike velocity as a function of time for atomistic simulation, magnetic levitation experiment, and continuum simulation as shown in Fig.1. The dashed lines indicate the slopes, from which the growth coefficients α_S are determined. Whereas atomistic simulations and experiments undergo a breakup at $t = 12\tau$ and $t = 8\tau$, respectively, continuum simulations, after an initial phase where the growth is dominated by the initial perturbation spectrum, show no such effect. The horizontal lines indicate the average terminal velocities for atomistic simulations and experiments. The inset shows the instantaneous α_S value $\frac{h^2}{4Ag h}$ (23). For all three methods, the penetration depth was measured as the point where the penetrating fluid reached 1 percent or 5 percent number fraction. The experimental data was omitted for $t > 18\tau$ due to boundary effects. In order to compare the α_S at different Atwood numbers $A=0.67, 0.29$, and 0.5 for atomistic simulations, experiments, and continuum simulations, respectively, the corresponding α_B are calculated (by using the experimental ratio of α_S/α_B) to 0.068 (atomistic), 0.055 (experiments), and 0.034 (continuum). Note that α_S increases with A , whereas α_B is constant (16,20).

Fig. 3. Initial conditions. Differences between spikes developing from a flat interface (top row: experiment, horizontal white bar corresponds to 1 cm; third row: atomistic simulation) and from an interface perturbed with a single mode (second row: experiment; fourth row: atomistic simulation).

Experimentally, the interface was given a single-mode perturbation by introducing a pair of sinusoidal, weakly magnetically permeable wires adjacent to the magnetically levitated interface. This perturbation had an amplitude to wavelength ratio $A_0/\lambda_0=0.0030$, and the experiment had an Atwood number $A=0.29$. The perturbed atomistic simulation ($A=0.67$) had $A_0/\lambda_0=0.0036$.

The continuum simulations (24,31) ($A=0.5$) were started with a small multimode perturbation spectrum centered on $0.2 \lambda_{max}$ (row 5), a small multimode perturbation spectrum centered on $0.2 \lambda_{max}$ added to a single mode ($A_0/\lambda_0=0.0036$, row 6), and a small multimode perturbation spectrum centered on $0.4 \lambda_{max}$ plus a single mode ($A_0/\lambda_0=0.0036$, row 7).

Perturbations initially boost the growth and introduce some order to the flow structure. However, later the influence of perturbations gets weaker. The single-mode perturbation was placed in all cases at $\sim 2 \lambda_{max}$. (The atomistic DSMC and continuum simulation frames shown here are a small subset of the whole simulation domain.)



Funding Acknowledgments

- Department of Energy, National Nuclear Security Administration, Advanced Simulation and Computing Program
- Los Alamos National Laboratory Directed Research and Development Program
- National Aeronautics and Space Administration